nature COMMUNICATIONS

ARTICLE

Received 1 Aug 2014 | Accepted 10 Nov 2014 | Published 16 Dec 2014

DOI: 10.1038/ncomms6806

Widom line and dynamical crossovers as routes to understand supercritical water

P. Gallo[1], D. Corradini[2,†] & M. Rovere[1]

Supercritical water is fundamental in many fields of applications and a precise characterization of the supercritical state is of uttermost importance for this liquid. In a fluid, when moving from the critical point into the single-phase region, the thermodynamic response functions show maxima reminiscent of the critical divergence. Here we study the thermodynamic properties of water in the supercritical region by analysing both available experimental data and our computer simulation results. We find that the lines connecting the maxima of the response functions converge on approaching the critical point in a single line, the Widom line. We further show that the Widom line coincides with a crossover from a liquid-like to a gas-like behaviour clearly visible in the transport properties. These thermodynamic and dynamic features show that the supercritical state in water is far more complex than what was so far believed, indicating a new perspective in the characterization of the thermodynamics of this state.

[1] Dipartimento di Matematica e Fisica, Universita' Roma Tre, via della Vasca Navale 84, I-00146 Rome, Italy. [2] Center for Polymer Studies and Department of Physics, Boston University, 590 Commonwealth Avenue, Boston, Massachusetts 02215, USA. † Present address: Sorbonne Universités, UPMC Univ Paris 06, UMR 8234, PHENIX, Paris, France; CNRS, UMR 8234, PHENIX, Paris, France. Correspondence and requests for materials should be addressed to P.G. (email: gallop@fis.uniroma3.it).

The coexistence between the gas and the liquid phases of a system terminates in a critical point, determined by the critical temperature T_C and pressure P_C. Beyond this point, for temperatures $T > T_C$ and pressures $P > P_C$ the two phases merge in a single supercritical fluid phase where gas and liquid are considered indistinguishable.

Supercritical fluids are present in nature, for instance, in submarine volcanoes or in atmospheres of giant planets. Among the different fluids, the study of thermodynamic, structural and dynamical properties of water in the supercritical phase plays the most crucial role in chemical engineering, in carbon capture and storage, in pharmaceutics, in waste disposal and in several other areas of applications[1,2] such as gasification of biomasses[3,4]. The studies of the supercritical region have been so far limited by technical difficulties in experiments, but the investigation of supercritical water is of great interest for understanding its physical properties[5,6]. The range of the supercritical region extends for $T > T_C$ and $P > P_C$, where $T_C = 647.096$ K and $P_C = 220.640$ bar, and it is upper bounded by the melting line between supercritical water and high pressure ice of type VII[7,8].

It is well known that water shows many peculiar features in all its phases and a great effort has been devoted to the study of this system in the thermodynamic space from ambient conditions down to crystallization/vitrification and up in temperature to the liquid–gas transition[9,10]. The challenge in this field is to find unifying concepts that can be used to describe the behaviour of water in the different phases, including the supercritical phase. In this context is the concept of Widom line (WL)[5] is particularly useful.

The concept of WL came to the fore in the last few years where it was extensively considered in supercooled water in connection with the possible existence of a liquid–liquid transition terminating in a second critical point[11–22].

In a fluid, when moving from the critical point to the single-phase region, it is expected that the correlation length keeps a maximum reminiscent of the critical divergence. On approaching the critical point from this region, quantities such as the specific heat and the isothermal compressibility show maxima that are expected to merge on a pseudo-critical single line terminating at the critical point. The maxima of those response functions collapse on the same line on approaching the critical point, as they become proportional to power laws of the correlation length. This line, called the WL, has been introduced to define this locus of maxima extending from the critical point into the single-phase region[5]. Entering into the single-phase region, the maxima are smeared out progressively and their values decrease.

The WL of supercritical noble gases, Lennard–Jones and van der Waals fluids was recently studied by experiments and simulations[23–27]. In particular, a recent experimental work has paved the way to a more profound knowledge of hot dense fluids by detecting a crossover in sound velocity of supercritical fluids of noble gases connected to the WL[26].

Moreover, in the case of water the existence and range of persistence of the WL in the supercritical state can be of great interest, as it can indicate the limiting pressure and temperature values for which the dissolving ability of supercritical water and its other technological important features can be exploited.

In this work, we show that the WL does exist in supercritical water and we identify its exact location in the phase diagram. Besides, we demonstrate that there is also a dynamic crossover on crossing the WL that witnesses the strict connection between dynamics and thermodynamics in supercritical water similar to that found for supercritical noble gases[26]. We also determine the range of temperatures above the liquid–gas critical point (LGCP), for which all thermodynamic and dynamic quantities converge on a single WL.

Results

Thermodynamic properties in the supercritical region. To identify the WL, we did analyse available data obtained from IAPWS-95/IAPS-85 equation of states (EoS), based on experimental data (see Methods), and we performed molecular dynamics simulations with the TIP4P/2005 potential[28]. We chose to use the TIP4P/2005, because among all atom models of that kind it gives the critical temperature and density closest to the experimental findings[29]. The values of the critical parameters from experiments are $T_C = 647.096$ K, $P_C = 220.640$ bar

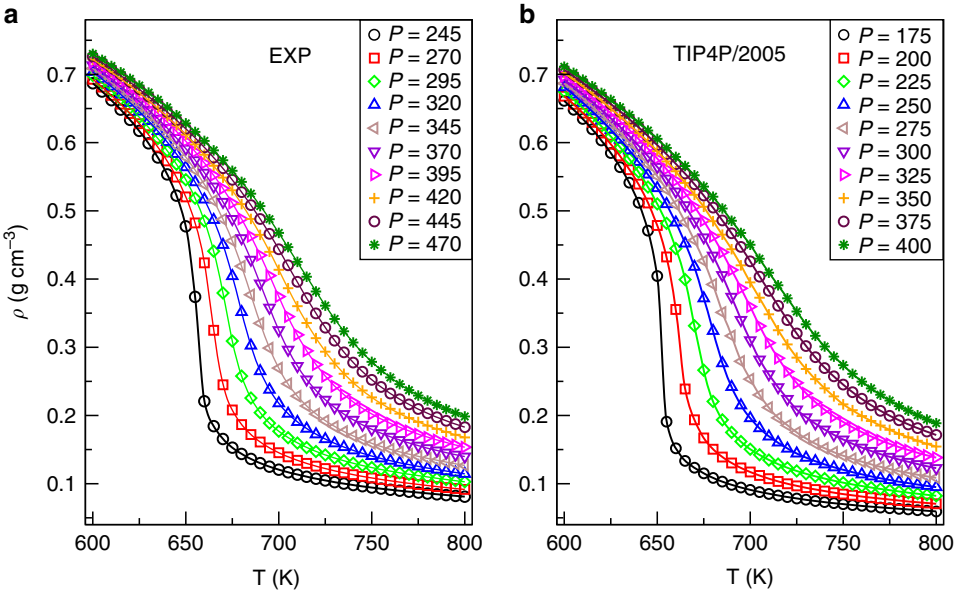

Figure 1 | Supercritical isobars from experiments and TIP4P/2005. (**a**) Isobars for experimental water between 600 and 800 K, and for pressures $P_n = 220 + 25n$ bar ($n = 1,...,10$). (**b**) Isobars for the TIP4P/2005 between 600 and 800 K, and for pressures $P_n = 150 + 25n$ bar ($n = 1,...,10$). In both panels, each colour corresponds to the same n in the formulas for the pressure, and as such it indicates the same distance from the respective critical point. The lines are obtained by spline interpolations.

and $\rho_C = 0.322\,g\,cm^{-3}$ and TIP4P/2005 gives $T_C = 640\,K$, $P_C = 146\,bar$ and $\rho_C = 0.31\,g\,cm^{-3}$.

In Fig. 1a we present the experimental isobars of water in the supercritical region, while in Fig. 1b we show the isobars calculated for the TIP4P/2005 potential. In both cases, the isobars are shown for temperatures between $T = 600\,K$ and $T = 800\,K$, and for pressures approximately at the same distance from the respective critical values: $P_n = 220 + 25n\,bar$ for experimental water and $P_n = 150 + 25n\,bar$ for TIP4P/2005 water, with $n = 1,...,10$. As such, these isobars span a zone of the $P-T$ diagram that goes from the liquid region to the supercritical region. Furthermore, the selected isobars never cross the liquid–gas coexistence line and therefore discontinuous jumps are not to be expected. Looking at Fig. 1a,b, we immediately note that the TIP4P/2005 model reproduces extremely well the envelope of the experimental isobars, albeit with the shift in pressure.

To find the location of the WL, we determined for both experimental and simulation data the maxima of three thermodynamic response functions. The constant pressure-specific heat C_P defined as

$$C_P = \frac{1}{N}\left(\frac{\partial H}{\partial T}\right)_P, \quad (1)$$

where H is the enthalpy. The expansion coefficient α_P defined as

$$\alpha_P = -\frac{1}{\rho}\left(\frac{\partial \rho}{\partial T}\right)_P, \quad (2)$$

and the isothermal compressibility K_T defined as

$$K_T = \frac{1}{\rho}\left(\frac{\partial \rho}{\partial P}\right)_T. \quad (3)$$

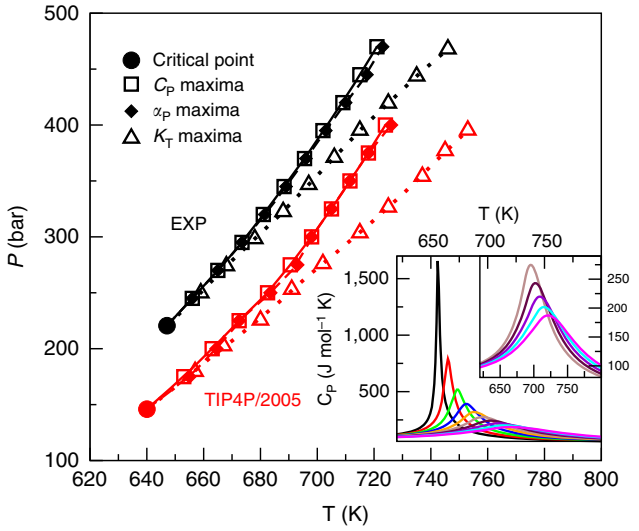

Figure 2 | The Widom lines from experiments and TIP4P/2005. Main Frame: critical points (circle) and $P-T$ location of the maxima of C_P (squares), α_P (diamonds) and K_T (triangles) as reproduced by experimental data (black) and by the molecular dynamics simulations performed using the TIP4P/2005 model (red). The definitions of the functions are provided in the text. All maxima were calculated along isobars. Lines are guides for the eye. Values for the critical point are respectively: from experiments $T_C = 647.096\,K$, $P_C = 220.640\,bar$ and $\rho_C = 0.322\,g\,cm^{-3}$ and from computer simulations $T_C = 640\,K$, $P_C = 146\,bar$ and $\rho_C = 0.31\,g\,cm^{-3}$. Inset: experimental isobaric specific heat C_P as a function of temperature for pressures $P_n = 220 + 25n\,bar$ ($n = 1,...,10$) above the critical pressure. The sub-inset shows a magnification for pressures $P \geq 370\,bar$. The lines are obtained directly from the linear interpolation of the data with $\Delta T = 1\,K$.

The behaviour of C_P is shown in the inset of Fig. 2 as extracted from experimental data for pressures above the LGCP. In spite of the fact that we are in the one-phase region, the specific heat peak is very well defined also for pressure that are quite far from the LGCP. The same persistence of defined maxima well above the LGCP is found also in simulations and for α_P and K_T (not shown).

The maxima of C_P, α_P and K_T are reported for both experiments and simulations in the main frame of Fig. 2. As the most important finding we note that both for the experimental data and for the simulation data, the C_P, α_P and K_T lines perfectly coincide in a certain range above the LGCP as expected from the theoretical interpretation of the WL. We do see that this range extends circa 30 K and 90 bar above the LGCP for both experiments and simulations. Further away from the LGCP C_P and α_P lines keep on coinciding, while K_T deviates. Apart from the small shift to lower pressures of the LGCP position, the agreement between the TIP4P/2005 and experiments for C_P, α_P and K_T lines is remarkable.

Transport properties in the supercritical region. We consider now the transport properties in the supercritical region.

The more extended experimental results for water in the supercritical range have been found for the viscosity η, which is reported in Fig. 3a. In the plot, we also marked the values of η corresponding to the P- and T-values of the experimental WL defined in the previous section. When the curves defining the WL start to separate, we marked the η corresponding to the maxima of the isobaric specific heat.

It is known that η at the critical point has a power law divergence with a small exponent[30,31]. The curves of η in the supercritical zone on approaching the critical pressure show a reminiscence of the critical behaviour with an almost vertical change with temperature.

The WL signs a change of behaviour of the viscosity from liquid like to gas like. In fact, in the liquid-like portion, all curves show a strong decrease of viscosity with temperature. In the gas-like portion, the change of slopes is more mild.

We note that at low densities the viscosity increases with temperature as predicted by theoretical approaches[32]. The increase is well fitted at low pressures by the formula for the viscosity in the dilute gas limit[31] as shown in Fig. 3a. At increasing pressure, the dense water gas far from the dilute limit shows a change of trend and the viscosity mildly decreases with temperature.

The diffusion coefficient D of supercritical water calculated with the molecular dynamics simulation of TIP4P/2005 is shown in Fig. 3b. Moreover, in the plot of the diffusion coefficient we did mark the values of D corresponding to the P- and T-values of the TIP4P/20005 WL defined in the previous section. When the curves defining the WL start to separate, we marked the D corresponding to the maxima of the isobaric specific heat.

In approaching the critical pressure, the variations of the diffusion coefficient become more drastic. The curves remain continuous as expected in the supercritical region, but at the lower pressures they show a strong change of slope close to the WL.

In simulations, the WL appears to mark a change in the behaviour of dynamics as well. For the lowest pressures, it is possible to distinguish between a gas-like and a liquid-like behaviour of the diffusion coefficient with the use of the Arrhenius formula

$$D = D_0 e^{-E_A/k_B T} \quad (4)$$

where E_A is the activation energy. The fits are shown in the inset

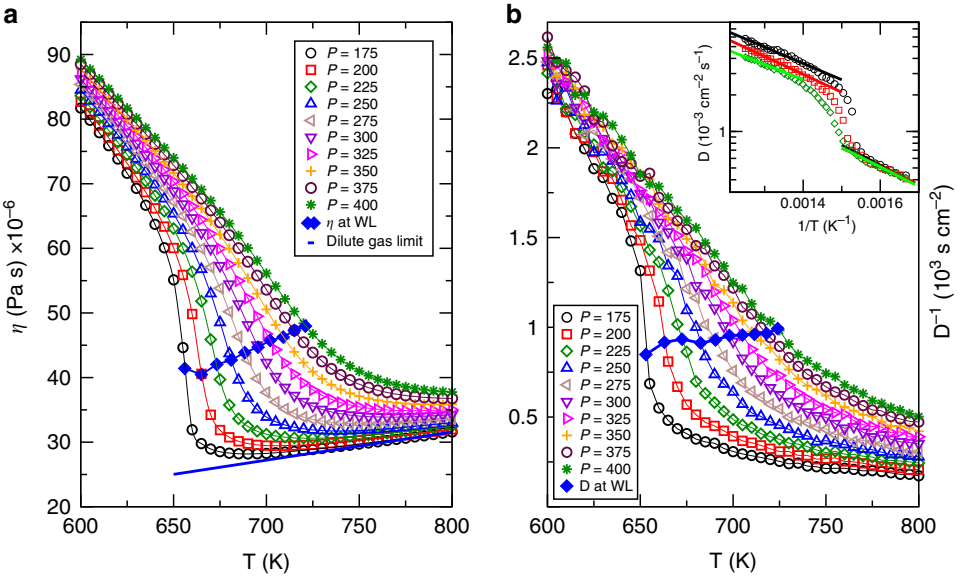

Figure 3 | Viscosity from experiments and diffusion coefficient from simulations. (**a**) Viscosity from experiments for different pressures (in bar). The curves are interpolations of the data and the diamonds are the values of η interpolated at the points of experimental WL and/or C_p maxima. The bold line is the viscosity in the dilute gas limit[31]. (**b**) Diffusion coefficients as obtained from simulations with the TIP4P/2005 potential along the isobars (the lines are guides for the eyes). The diamonds are the values of D interpolated at the points of WL and/or C_p maxima given by the model and reported in Fig. 2. In the inset, the coefficient D for the lowest pressures are reported as function of $1/T$; the bold lines are the fitting with the equation (4); the activation energies are: for high T, $E_A = 25.7\,\mathrm{kJ\,mol^{-1}}$ for $P = 175$ bar, $E_A = 28.2\,\mathrm{kJ\,mol^{-1}}$ for $P = 200$ bar, $E_A = 23.8\,\mathrm{kJ\,mol^{-1}}$ for $P = 225$ bar; for low T, $E_A = 31.5\,\mathrm{kJ\,mol^{-1}}$ for $P = 175$ bar, $E_A = 28.7\,\mathrm{kJ\,mol^{-1}}$ for $P = 200$ bar, $E_A = 30.8\,\mathrm{kJ\,mol^{-1}}$ for $P = 225$ bar.

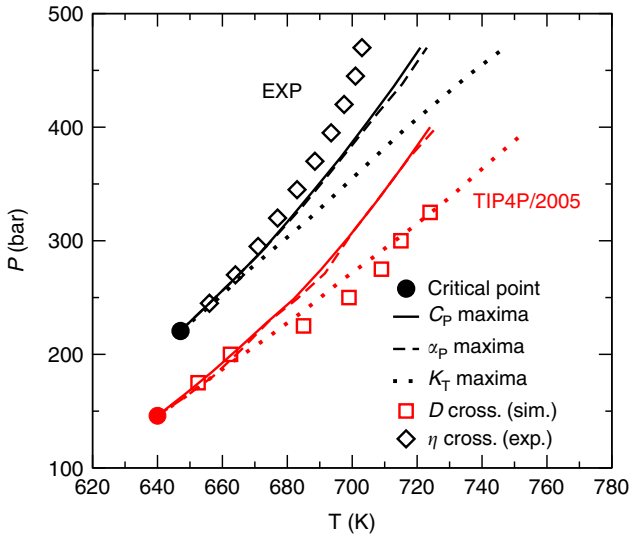

Figure 4 | Dynamic crossover at the Widom line. The (P, T) location of the viscosity crossovers extracted from experimental data and of diffusion coefficient crossovers extracted from TIP4P/2005 are shown in the figure together with LGCP and thermodynamic response functions maxima from experiments and simulations.

of the top part of Fig. 3b. For temperatures far from the critical point at the lowest pressures, the diffusion in both the gas-like and in the liquid-like regions is determined by activated processes with different activation energies. The values of E_A are reported in the figure caption and they result to be higher in the liquid-like part.

For pressures higher than $P = 250$ bar, it becomes more difficult to realize a good fit for the diffusion.

From the behaviour of the experimental η and the simulated D, we can extract the points where the curvature changes. To precisely locate the inflection points, we calculated the numerical derivatives of the curves (not shown).

We now present the lines calculated at the P- and T-values of the inflection points for both the experimental η and the calculated D, together with the maxima of C_P, α_P and K_T for both experiments and simulations in Fig. 4.

It is evident that similar to the thermodynamic response functions, the lines of the dynamic crossovers located through the derivatives of η and D coincide with the WL in approaching the critical point. In particular, the crossover of the experimental viscosity follows the WL for almost 30 K. It is clear from this results that the transport properties of supercritical water are strongly affected by the presence of the WL.

Discussion

We consider the thermodynamic properties of water along the isobars in the supercritical region analysing experimental results and calculations obtained from the TIP4P/2005 model for water. We derive for both experiments and simulations the lines of the maxima of C_P, K_T and α_P in the single-phase region above the critical point. These curves are related to the WL, defined as the line of the maxima of the correlation length. Starting from (T_C and P_C), we find that the curves of the C_P, α_P and K_T maxima coincide in the (T, P) plane for a range of circa 30 K and 90 bar, thus following the WL. For higher temperatures and pressures, the C_P and α_P maxima follow a similar path, while the maxima of K_T deviate.

Importantly, we test that the WL coincides with a crossover from a liquid-like to a gas-like behaviour witnessed by a crossover in dynamics of viscosity and diffusion coefficient.

These results show analogies with the simulation studies of the WL of supercooled water where dynamical changes[11,33–35] and structural changes[18] appear on crossing the WL. In particular, for supercooled TIP4P/2005 water it has been shown that the WL corresponds to having equal occurrence of the two local

structures, high-density liquid and low-density liquid, involved in the fluctuations[36].

We therefore show that the supercritical state of water can be divided into a gas-like region and a liquid-like region by the WL anticipating the phase separation and the coexistence that is found below the critical point. These results are in line with recent experimental findings on supercritical noble gases[26,27], and together with those indicate a new perspective in the characterization of the fluid–matter thermodynamics of the supercritical state of water and possibly of other liquids with all the important consequences that this can have for many areas of application. The supercritical state cannot, in fact, be considered as an indistinguishable fluid phase any longer.

In the future, it would be interesting to extend the study to other water models and to explore with simulations other dynamical and structural features of supercritical water. In noble gases, there is in particular a vivid debate[27,37] on whether a dynamical line, called the Frenkel line, can be of use to characterize regions of different dynamical behaviour in the supercritical state. This line is defined as a crossover in positive sound dispersion corresponding to loss of shear stiffness of the liquid and it has been shown to lie, with respect to the WL, in the liquid-like side of supercritical noble gases[37,38]. It would be interesting to explore the behaviour of this line in a molecular and network forming liquid, like water.

Besides, it would be of great relevance also to extend the present study to other fluids such as CO_2 whose supercritical state is of uttermost importance in green chemistry.

Methods

Experimental data. The data on supercritical water are obtained from the IAPWS-95/IAPS-EoS, based on experimental data. The EoS is provided by the NIST Chemistry WebBook, at the site http://webbook.nist.gov/chemistry/fluid/.

Computer simulation model. We performed simulations using the TIP4P/2005 model for water. TIP4P/2005 (ref 28) is a re-parametrized version of the 'classical' TIP4P model[39] and it is widely employed. In particular, it was shown to be the best rigid and non-polarizable potential for the reproduction of many features of experimental water[29].

Method of simulation. Molecular dynamics simulations were performed in a cubic box containing 4,096 water molecules with an initial density $\rho = 1.0\,\mathrm{g\,cm^{-3}}$. For each pressure, we first equilibrate the system at each temperature for 0.1 ns and then execute production runs of 1 ns from $T = 600$ K to $T = 800$ K, with $\Delta T = 5$ K. The simulated isobars are for pressures $P_n = 150 + 25n$ bar ($n = 1,...,10$). As the critical pressure of the TIP4P/2005 model is $P_c = 146$ bar, our isobars never cross the liquid–gas first-order phase transition line. The simulations are run in the *NPT* ensemble, with a time step for the integration of the equation of motion of 1 fs. We control the temperature using the Nosé–Hoover thermostat[40,41] and the pressure by the Parrinello–Rahman barostat[42,43]. The short-range interactions are cut off at 1 nm. The electrostatics is dealt with by using the Particle Mesh Ewald algorithm. The simulations are run using GROMACS (versions 4.5.3 and 4.5.5)[44]. For the calculation of the diffusion coefficient, the first and the last 10% of the run are excluded from the linear fit of the mean square displacement.

References

1. Akiya, N. & Savage, P. E. Roles of water for chemical reactions in high-temperature water. *Chem. Rev.* **102,** 2725–2750 (2002).
2. *NATO Science Series E: Applied Science* (eds Kiran, J., Debenedetti, P. G. & Peters, J.) 366 (Kluwer, 2000).
3. Huelsman, C. M. & Savage, P. E. Reaction pathways and kinetic modeling for phenol gasification in supercritical water. *J. Supercrit. Fluids* **81,** 200–209 (2013).
4. Savage, P. E. Organic chemical reactions in supercritical water. *Chem. Rev.* **99,** 603–622 (1999).
5. McMillan, P. F. & Stanley, H. E. Going supercritical. *Nat. Phys.* **6,** 479–480 (2010).
6. Wernet, P. *et al.* Spectroscopic characterization of microscopic hydrogen-bonding disparities in supercritical water. *J. Chem. Phys.* **123,** 154503 (2005).
7. Lin, J. F. *et al.* High pressure-temperature Raman measurements of H2O melting to 22 GPa and 900 K. *J. Chem. Phys.* **121,** 8423–8427 (2004).
8. Kimura, T., Kuwayama, Y. & Yagi, T. Melting temperatures of H2O up to 72 GPa measured in a diamond anvil cell using CO2 laser heating technique. *J. Chem. Phys.* **140,** 074501 (2014).
9. Franks, F. *Water: a Matrix for Life* Second Edition (Royal Society of Chemistry, 2000).
10. Debenedetti, P. G. Supercooled and glassy water. *J. Phys. Condens. Matter* **15,** R1669–R1726 (2003).
11. Xu, L. *et al.* Relation between the Widom line and the dynamic crossover in systems with a liquid-liquid phase transition. *Proc. Natl Acad. Sci. USA* **102,** 16558–16562 (2005).
12. Franzese, G. & Stanley, H. E. The Widom line of supercooled water. *J. Phys. Condens. Matter* **19,** 205126 (2007).
13. Huang, C. *et al.* The inhomogeneous structure of water at ambient conditions. *Proc. Natl Acad. Sci. USA* **106,** 15214–15218 (2009).
14. Mallamace, F. *et al.* Evidence of the existence of the low-density liquid phase in supercooled, confined water. *Proc. Natl Acad. Sci. USA* **104,** 424–428 (2007).
15. Abascal, J. L. F. & Vega, C. Widom line and the liquid-liquid critical point for the TIP4P/2005 water model. *J. Chem. Phys.* **133,** 234502 (2010).
16. Fuentevilla, D. A. & Anisimov, M. A. Scaled equation of state for supercooled water near the liquid-liquid critical point. *Phys. Rev. Lett.* **97,** 195702 (2006).
17. Banerjee, D., Bhat, S. N., Bhat, S. V. & Leporini, D. ESR evidence for 2 coexisting liquid phases in deeply supercooled bulk water. *Proc. Natl Acad. Sci. USA* **106,** 11448–11453 (2009).
18. Wikfeldt, K. T., Huang, C., Nilsson, A. & Pettersson, L. G. M. Enhanced small-angle scattering connected to the Widom line in simulations of supercooled water. *J. Chem. Phys.* **134,** 214506 (2011).
19. Corradini, D., Rovere, M. & Gallo, P. A route to explain water anomalies from results on an aqueous solution of salt. *J. Chem. Phys.* **132,** 134508 (2010).
20. Xu, L., Buldyrev, S. V., Angell, C. A. & Stanley, H. E. Thermodynamics and dynamics of the two-scale spherically symmetric Jagla ramp model of anomalous liquids. *Phys. Rev. E* **74,** 031108 (2006).
21. Corradini, D., Buldyrev, S. V., Gallo, P. & Stanley, H. E. Effects of hydrophobic solutes on the liquid-liquid critical point. *Phys. Rev. E* **81,** 061504 (2010).
22. Corradini, D., Su, Z., Stanley, H. E. & Gallo, P. A molecular dynamics study of the equation of state and structure of supercooled aqueous solutions of methanol. *J. Chem. Phys.* **137,** 184503 (2012).
23. Brazhkin, V. V., Fomin, Y. D., Lyapin, A. G., Ryzhov, V. N. & Tsiok, E. N. Widom line for the liquid-gas transition in Lennard-Jones system. *J. Phys. Chem. B* **115,** 14112–14115 (2011).
24. Brazhkin, V. V. & Ryzhov, V. N. Van der Waals supercritical fluid: exact formulas for special lines. *J. Chem. Phys.* **135,** 084503 (2011).
25. Gorelli, F., Santoro, M., Scopigno, T., Krisch, M. & Ruocco, G. Liquidlike behavior of supercritical fluids. *Phys. Rev. Lett.* **97,** 245702 (2006).
26. Simeoni, G. G. *et al.* The Widom line as the crossover between liquid-like and gas-like behaviour in supercritical fluids. *Nat. Phys.* **6,** 503–507 (2010).
27. Gorelli, F. A. *et al.* Dynamics and Thermodynamics beyond the critical point. *Sci. Rep.* **3,** 1203 (2013).
28. Abascal, J. L. F. & Vega, C. A general purpose model for the condensed phases of water: TIP4P/2005. *J. Chem. Phys.* **123,** 234505 (2005).
29. Vega, C. & Abascal, J. L. F. Simulating water with rigid non-polarizable models: a general perspective. *Phys. Chem. Chem. Phys.* **13,** 19663–19688 (2011).
30. Bhattacharjee, J. K., Ferrell, R. A., Basu, R. S. & Sengers, J. V. Crossover function for the critical viscosity of a classical fluid. *Phys. Rev. A* **24,** 1469–1475 (1981).
31. Sengers, J. V., Perkins, R. A., Huber, M. L. & Friend, D. G. Viscosity of H_2O in the critical region. *Int. J. Thermophys.* **30,** 374–384 (2009).
32. Chapman, S. & Cowling, T. G. *The Mathematical Theory of Non-uniform Gases, Cambridge Mathematical Library* Third Edition (Cambridge University Press, 1970).
33. Poole, P. H., Becker, S. R., Sciortino, F. & Starr, F. W. Dynamical behavior near a liquid-liquid phase transition in simulations of supercooled water. *J. Phys. Chem. B* **115,** 14176–14183 (2011).
34. Gallo, P. & Rovere, M. Mode coupling and fragile to strong transition in supercooled TIP4P water. *J. Chem. Phys.* **137,** 164503 (2012).
35. Picasso, G. C., Malaspina, D. C., Carignano, M. A. & Szleifer, I. Cooperative dynamic and diffusion behavior above and below the dynamical crossover of supercooled water. *J. Chem. Phys.* **139,** 044509 (2013).
36. Wikfeldt, K. T., Nilsson, A. & Pettersson, L. G. M. Spatially inhomogeneous bimodal inherent structure of simulated liquid water. *Phys. Chem. Chem. Phys.* **13,** 19918–19924 (2011).
37. Brazhkin, V. V., Fomin, Y. D., Lyapin, A. G., Ryzhov, V. N. & Trachenko, K. Two liquid states of matter: A dynamic line on a phase diagram. *Phys. Rev. E* **85,** 031203 (2012).

38. Brazhkin, V. V. *et al.* 'Liquid-gas' transition in the supercritical region: fundamental changes in the particle dynamics. *Phys. Rev. Lett.* **111,** 145901 (2013).
39. Jorgensen, W. L., Chandrasekhar, J., Madura, J. D., Impey, R. W. & Klein, M. L. Comparison of simple potential functions for simulating liquid water. *J. Chem. Phys.* **79,** 926–935 (1983).
40. Nosé, S. A molecular dynamics method for simulations in the canonical ensemble. *Mol. Phys.* **52,** 255–268 (1984).
41. Hoover, W. G. Canonical dynamics: equilibrium phase-space distributions. *Phys. Rev. A* **31,** 1695–1697 (1985).
42. Parrinello, M. & Rahman, A. Polymorphic transitions in single crystals: a new molecular dynamics method. *J. Appl. Phys.* **52,** 7182–7190 (1981).
43. Nosé, S. & Klein, M. L. Constant pressure molecular dynamics for molecular systems. *Mol. Phys.* **50,** 1055–1076 (1983).
44. Hess, B., Kutzner, C., van der Spoel, D. & Lindahl, E. GROMACS 4: algorithms for highly efficient, load-balanced, and scalable molecular simulation. *J. Chem. Theory Comp.* **4,** 435–447 (2008).

Acknowledgements

P.G. and M.R. acknowledge the computational support of the Roma Tre INFN-GRID.

Author contributions

All the authors contributed equally to the research and to the writing of the paper.

Additional information

Competing financial interests: The authors declare no competing financial interests.

How to cite this article: Gallo, P. *et al.* Widom line and dynamical crossovers as routes to understand supercritical water. *Nat. Commun.* 5:5806 doi: 10.1038/ncomms6806 (2014).